Application Note 29

Prism Compressor for Ultrashort Laser Pulses

Technology and Applications Center
Newport Corporation

Spectra-Physics
A Division of Newport Corporation

Newport®
Experience | Solutions

The Effect of Dispersion on Ultrashort Pulses

In the time domain, the electric field for a Gaussian pulse with a carrier frequency, ω_0, pulse duration, Δt, and phase, $\theta(t)$, can be described by,

$$E(t) = \sqrt{A_t e^{-\ln 2\left(\frac{2t}{\Delta t}\right)^2}}\, e^{-i(\omega_0 t + \theta(t))} + c.c. \qquad (1)$$

where c.c. denotes the complex conjugate. In this expression, A_t is the amplitude of the pulse, ω_0 determines the color of the pulse, Δt determines the minimum pulse duration and consequently the bandwidth of the pulse, and $\theta(t)$ determines the temporal relationship among the frequency components contained within the bandwidth of the pulse. $\theta(t)$ plays an important role in altering the pulse duration. It is the term that is responsible for pulse broadening in dispersive media and can be thought of as adding a complex width to the Gaussian envelope.

The description of the Gaussian pulse given by (1) is intuitive in the sense that it is fairly straightforward to conceptualize a pulse in the time domain. However, when dealing with pulses traveling through dispersive media, it can be problematic to work in the time domain. For example, in order to determine the duration of a pulse after traveling through some dispersive material, it is necessary to solve a convolution integral[1] which in general must be done numerically. However, due to the fact that convolutions become products upon a Fourier transformation[2], it is convenient to solve this type of problem in the frequency domain.

Time and frequency along with position and momentum represent a class of variables known as Fourier pairs.[2] Fourier pairs are quantities that can be interconnected through the Fourier transform. Performing a Fourier transform on equation (1) yields,

$$E(\omega) = \sqrt{A_\omega e^{-\ln 2\left(\frac{2(\omega-\omega_o)}{\Delta\omega}\right)^2}}\, e^{-i\varphi_{Pulse}(\omega-\omega_0)} \qquad (2)$$

(for the sake of brevity, negative frequency components are omitted). The electric field is now expressed as a function of frequency, $\Delta\omega$ and Δt are related through the uncertainty relation[1] $\Delta\omega\Delta t = 4\ln(2)$, and the spectral phase, $\varphi(\omega)$, describes the relationship between the frequency components of the pulse. In equation (2), ω as well as $\Delta\omega$ represent angular frequencies. Angular frequency can be converted to linear frequency, ν (i.e. the observable quantity), by dividing it by $2\pi, \nu = \frac{\omega}{2\pi}$. In terms of the linear frequency, the uncertainty principle is given by, $c_B = \Delta\nu\Delta t = \frac{2\ln(2)}{\pi}$. When an input pulse, $E_{in}(\omega)$, passes through a dispersive medium, the phase added by the material is given simply by the product of the input field with the transfer function of the material. The emerging pulse $E_{out}(\omega)$, is given by,

$$E_{out}(\omega) = E_{in}(\omega)R(\omega)e^{-i\varphi_{Mat}(\omega-\omega_0)} \qquad (3)$$

where $\varphi_{Mat}(\omega-\omega_0)$ is the spectral phase added by the material and $R(\omega)$ is an amplitude scaling factor which for a linear transparent medium can be approximated by, $R(\omega) \approx 1$.[1]

It is a common convention to express spectral phase as a Taylor expansion around the carrier frequency of the pulse as shown below,

$$\varphi(\omega-\omega_0) = \varphi_0 + \varphi_1\cdot(\omega-\omega_0) + \varphi_2\cdot\frac{(\omega-\omega_0)^2}{2} + \varphi_3\cdot\frac{(\omega-\omega_0)^3}{6} + \ldots \qquad (4)$$

This approach allows a more straightforward understanding of the effect of material dispersion on properties of the pulse. Taking into account that $\varphi(\omega) = k(\omega)L$, where k is the propagation constant, and L is the length of the medium, while also considering that the group velocity is defined as $\upsilon_G = d\omega/dk$, it is easy to see that first term in (4) adds a constant to the phase. The second term, proportional to $1/\upsilon_G$, adds delay to the pulse. Neither of these terms affects the shape of the pulse. The third term, referred to as group delay dispersion (GDD), is proportional to $\frac{d}{d\omega}\left(\frac{1}{\upsilon_G}\right)$, also known as group velocity dispersion (GVD). It introduces a frequency dependent delay of the different spectral components of the pulse, thus temporally changing it. The GDD and GVD are related through $\varphi_2(\omega) = k_2(\omega)L$. The fourth term, referred to as Third Order Dispersion (TOD) applies quadratic phase across the pulse. For the purpose of this note, we will truncate the series at the third term, GDD, only making references to higher order terms when necessary. Truncating equation (4) at the third term allows us to rewrite equation (3) for a Gaussian pulse as,

$$E_{out}(\omega) = \sqrt{A_\omega e^{-\ln 2\left(\frac{2(\omega-\omega_o)}{\Delta\omega}\right)^2}}\, e^{-i(\varphi_{2,Pulse}+\varphi_{2,Mat})\frac{(\omega-\omega_0)^2}{2}} \qquad (5)$$

hence phases in the frequency domain are simply additive. This result underscores the advantage of performing these types of calculations in the frequency domain.

To arrive at the new pulse duration, it is necessary to transform the spectral envelope of equation (5) back into the time domain. Performing this Fourier transform, the pulse envelope is given by,

$$E_{out}(t) = \sqrt{A_t'}\, e^{\frac{4(\ln 2)t^2}{2[\Delta t^2 + i4(\ln 2)\varphi_2]}} \qquad (6)$$

where φ_2 is the sum of the group delay dispersion of the material and the group delay of the pulse. In order to get the new pulse duration, Δt_{out}, it is necessary to obtain the intensity, $I_{out}(t)$, by squaring the electric field in equation (6) and then relating $I_{out}(t)$ to the general form for a Gaussian pulse,

$$e^{-\ln 2\left(\frac{2t}{\Delta t_{out}}\right)^2} = e^{\frac{4(\ln 2)t^2\Delta t^2}{\Delta t^4 + 16(\ln 2)^2{\varphi_2}^2}} \qquad (7)$$

Solving equation (7) for Δt_{out},

$$\Delta t_{out} = \frac{\sqrt{\Delta t^4 + 16(\ln 2)^2{\varphi_2}^2}}{\Delta t} \qquad (8)$$

provides an expression for the pulse duration. Finally, by solving equation (8) for group delay dispersion while replacing the transform limited pulse duration with the spectral bandwidth of the pulse, GDD can be expressed completely in terms of observables (i.e. pulse width and spectrum),

$$\varphi_2 = \frac{1}{4(\ln 2)}\sqrt{\left(\frac{c_B \Delta t_{out}}{\Delta \nu}\right)^2 - \left(\frac{c_B}{\Delta \nu}\right)^4} \qquad (9)$$

where $\Delta\nu = c\Delta\lambda/\lambda^2$. In general, c_B is a function of the pulse profile as shown in Table 1. It should be noted that equation (9) is strictly valid for Gaussian pulses.

Table 1. Time-bandwidth product C_B for various pulse profiles

Field Profile	Gaussian	Sech	Lorentzian	Rectangle
c_B	0.441	0.315	0.142	0.443

Dispersion in materials is defined by the group velocity dispersion. In order to estimate amount of GDD introduced by a material of length L, one has to calculate the wavelength dependent index of refraction, n(λ), typically in the form of a Sellmeier's type equation, and then calculate second derivative at the wavelength of interest. GVD is related to the second derivative of refractive index with respect to wavelength by $GVD = \frac{\lambda^3}{2\pi c^2}\left(\frac{d^2 n}{d\lambda^2}\right)$. GDD is simply a product of GVD with the length of the material. The dispersive properties of several optical materials are shown in Table 2.

Table 2. Material parameters for fused silica, LakL21, SF10 and BK7 glass

Material	λ (nm)	n(λ)	dn/dλ (μm^{-2})	d^{2}n/dλ^2 (μm^{-2})	d^{3}n/dλ^3 (μm^{-2})	GVD (fs^2/mm)	TOD (fs^3/mm)
Fused Silica	400	1.470	-0.1091	0.8609	-9.600	97.43	30.20
	450	1.466	-0.07577	0.5115	-4.984	82.43	27.24
	500	1.462	-0.05536	0.3230	-2.809	71.40	25.53
	550	1.460	-0.04218	0.2135	-1.686	62.82	24.62
	600	1.458	-0.03331	0.1462	-1.064	55.85	24.28
	650	1.457	-0.02716	0.1029	-0.6993	49.98	24.42
	700	1.455	-0.02278	0.07397	-0.4755	44.87	24.99
	750	1.454	-0.01961	0.05402	-0.3328	40.30	25.99
	800	1.453	-0.01728	0.03988	-0.2388	36.11	27.44
	850	1.453	-0.01556	0.02963	-0.1751	32.18	29.36
LakL21	400	1.659	-0.1788	1.463	-16.95	165.6	57.42
	450	1.652	-0.1226	0.8546	-8.552	137.7	49.42
	500	1.647	-0.08870	0.5340	-4.731	118.0	44.78
	550	1.643	-0.06698	0.3507	-2.804	103.2	42.05
	600	1.640	-0.05245	0.2393	-1.753	91.40	40.59
	650	1.637	-0.04239	0.1682	-1.144	81.68	40.06
	700	1.636	-0.03524	0.1210	-0.7740	73.37	40.30
	750	1.634	-0.03005	0.08855	-0.5395	66.06	41.25
	800	1.632	-0.02623	0.06567	-0.3858	59.46	42.89
	850	1.631	-0.02338	0.04914	-0.2821	53.37	45.25
SF10	400	1.778	-0.5434	5.946	-97.73	672.9	510.5
	450	1.757	-0.3346	2.899	-36.74	467.1	301.6
	500	1.743	-0.2253	1.632	-17.08	360.8	213.5
	550	1.734	-0.1610	1.006	-9.046	295.9	168.1
	600	1.727	-0.120 2	0.6595	-5.237	251.9	141.5
	650	1.721	-0.09280	0.4527	-3.235	219.8	124.7
	700	1.717	-0.07367	0.3218	-2.100	195.2	113.6
	750	1.714	-0.05989	0.2352	-1.418	175.5	106.1
	800	1.711	-0.04970	0.1759	-0.9885	159.2	101.1
	850	1.709	-0.04201	0.1339	-0.7081	145 .5	97.97
BK7	400	1.529	-0.1303	1.082	-12.30	122.4	40.20
	450	1.524	-0.08858	0.6384	-6.262	102.9	34.72
	500	1.520	-0.06312	0.4029	-3.485	89.07	31.31
	550	1.517	-0.04665	0.2676	-2.074	78.74	29.02
	600	1.515	-0.03549	0.1851	-1.301	70.69	27.39
	650	1.514	-0.02765	0.1322	-0.8510	64.22	26.19
	700	1.513	-0.02197	0.09709	-0.5764	58.89	25.28
	750	1.512	-0.01776	0.07294	-0.4021	54.42	24.57
	800	1.511	-0.01456	0.05589	-0.2877	50.60	24.01
	850	1.510	-0.01209	0.04356	-0.2103	47.31	23.55

By measuring the spectrum and autocorrelation for a Gaussian pulse, equation (9) can be used to determine the amount of GDD. Figure 1 illustrates the results of a numerical simulation of the electric field for three pulses, all containing 100 nanometers of bandwidth, centered around 800 nanometers. The black curve corresponds to a pulse with the GDD set to zero, the red curve corresponds to a pulse with the GDD set to 5 fs^2 and the blue curve corresponds to a pulse with the GDD set to -5 fs^2. The pulse with the minimum time duration corresponds to the pulse having zero GDD. For the red pulse (positive chirp), the higher frequency components are lagging behind the lower ones and for the blue pulse (negative chirp), the lower frequency components are lagging behind the higher ones.

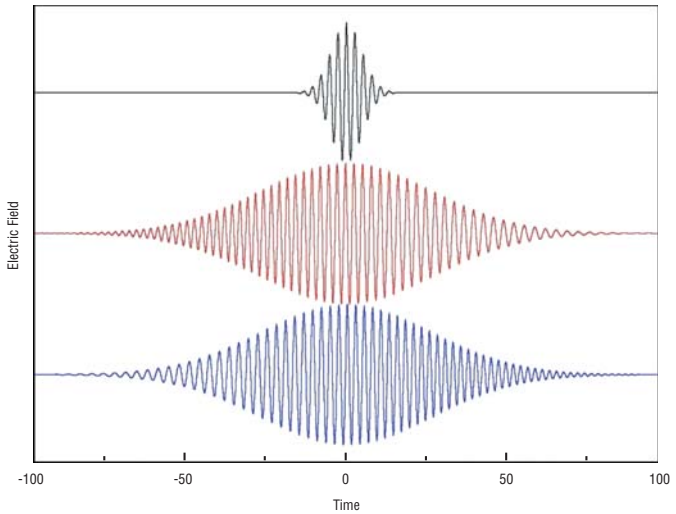

Figure 1. The effect of GDD on pulse with 100 nm bandwidth

Figure 2 shows the width of a Gaussian pulse at 800nm before and after propagation through 20 mm of BK7 glass calculated using equation (8) and data from Table 2.

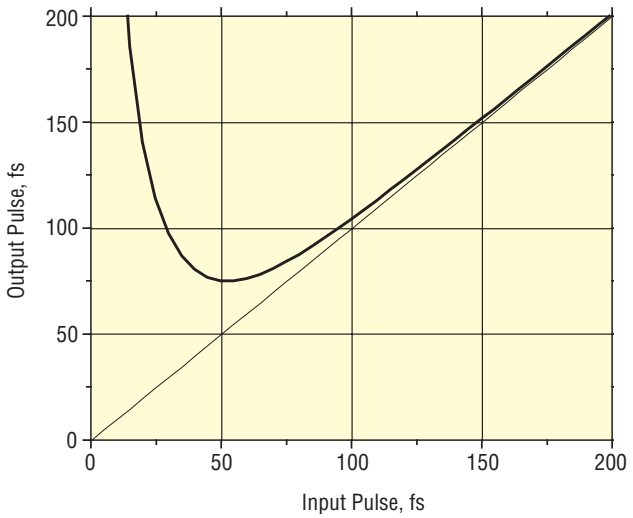

Figure 2. Broadening of a femtosecond ulse at 800 nm after propagation through 20 mm of BK7

The amount of introduced GDD in this case is about 1000 fs^2, and is equivalent to propagating the beam through only a few optical components. It is clear that the effect is not significant for pulses longer than 100 fs. However, a 25 fs pulse broadens by a factor of 4.

Dispersion Compensation Using a Prism Compressor

How can we compensate for the chirp acquired by a femtosecond pulse after propagation through a dispersive material? Angular dispersion produces negative GDD which may be introduced either through a sequence of prisms or gratings.[1,3,4,5] This note describes a simple and cost effective prism compressor suitable for compensation of GDD typical for common femtosecond setups based on oscillators, amplifiers and OPAs.

The unfolded geometry of the prism compressor consists of a four prism sequence as shown in Figure 3. The apex angle of each prism is equal to Brewster angle for a given wavelength and the prisms are arranged in such a way that the beam enters and exits each prism under Brewster angle. The reflection losses in that case are minimized for the P polarization. The first prism disperses the beam.

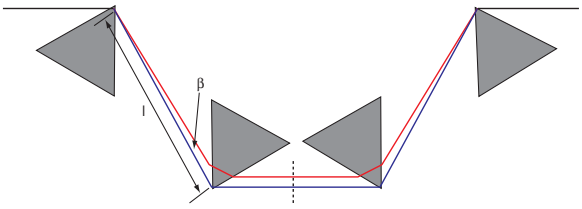

Figure 3. Geometrical arrangement of a four prism sequence for introducing negative GDD

The second prism collimates the dispersed beam. The third and fourth prisms undo the action of the first two such that the beams entering and exiting the compressor are spatially identical. The dashed line in Figure 3 represents a folding mirror which can be placed after the second prism and utilize two prisms instead of four in double pass geometry. It can be shown that a wavelength dependent path length, P(λ), due to dispersion is given by,

$$P = 2l\cos\beta \qquad (10)$$

where l is the distance between apex 1 and apex 2 of the first two prisms and β is the angle of the dispersed beam after the first prism.[4] The GDD introduced by the prism sequence is given by,

$$GDD_{PRISM} = \left(\frac{\lambda^3}{2\pi c^2}\right)\frac{d^2P(\lambda)}{d\lambda^2} \qquad (11)$$

where λ is the wavelength of light and c is the speed of light. Utilizing the approach of Fork et al[4]., equation (11) can be written as,

$$GDD_{PRISM} = \frac{\lambda^3}{2\pi c^2}\left[4l\left\{\left[\frac{d^2n}{d\lambda^2}+\left(2n-\frac{1}{n^3}\right)\left(\frac{dn}{d\lambda}\right)^2\right]\sin\beta - 2\left(\frac{dn}{d\lambda}\right)^2\cos\beta\right\}+4\left(\frac{d^2n}{d\lambda^2}\right)\left(2D_{1/e^2}\right)\right] \qquad (12)$$

where n is the refractive index and $D_{1/e}$ is the beam diameter at $1/e^2$. The refractive index as well as the derivatives of the refractive index can be readily obtained from Sellmeier's equations for a given material (see Table 2) and β can be estimated from,

$$\beta \approx -2\frac{dn}{d\lambda}\Delta\lambda \qquad (13)$$

Since β is relatively small and sin(β)<<cos(β) one can simplify Eq.(12) as,

$$GDD_{PRISM} \approx \frac{\lambda^3}{2\pi c^2}\left[-4l\left\{2\left(\frac{dn}{d\lambda}\right)^2\right\}+4\left(\frac{d^2n}{d\lambda^2}\right)\left(2D_{1/e^2}\right)\right] \qquad (14)$$

The first term is always negative and depends on prism separation. The second term is always positive and depends on the pathlength through the prisms. Varying the prism separation and the pathlength through the prisms one can control the sign and the amount of introduced dispersion. It should be noted, however, that at 800 nm for SF10 glass prisms, the sin(β) term in (12) introduces a 20% correction factor to the GDD for 50 nanometers of bandwidth. For that reason all calculations in this note were performed using the exact equation (12).

Building the Compressor

The experimental setup for the pulse compression is shown in Figure. 4. The compressor can be set up as follows:

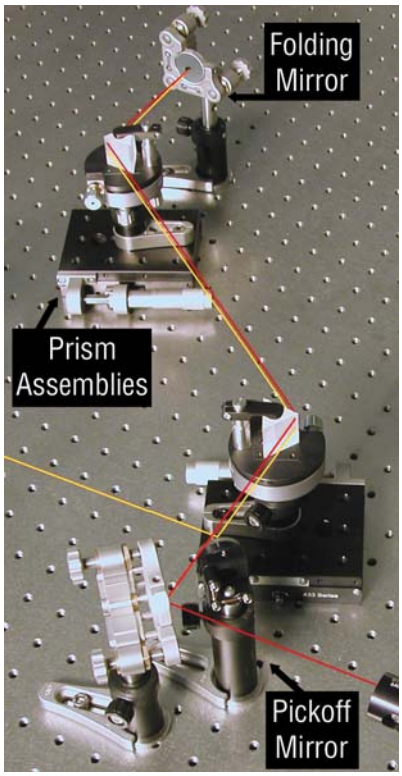

Figure 4. Experimental setup of the two-prism compressor

1 Determine the GDD responsible for elongating the pulse. This can be accomplished by measuring the spectrum and autocorrelation width, and then calculating the GDD from equation (9).

2. Determine the transform limited pulse duration Δt corresponding to the measured bandwidth from $\Delta t = \frac{c_B \lambda^2}{c \Delta \lambda}$. At 800 nm this expression simplifies to $\Delta t(fs) \approx \frac{940}{\Delta \lambda(nm)}$. This in conjunction with wavelength will be the primary determinants of the prism material. As a rule of thumb, SF10 can be used for pulse durations greater than 50 fs as long as the wavelength is above 400 nm. LakL21 can be used for pulses greater than 25 fs at wavelengths longer than 380 nm. Fused silica should be reserved for pulses shorter than 25 fs and wavelengths shorter than 380 nm.

3. Use data from Table 2 (first and second derivatives of refractive index) and solve equation (12) to determine the prism separation necessary to balance the positive GDD on the pulse for a given wavelength. Tables of prism distances for certain wavelengths are provided in Appendix 1, along with a guide explaining the proper use of these tables.

4. Assemble the Prism Assemblies as shown in Figure 5.

5. Prior to inserting the Prism 1 Assembly in the beam path, take care to ensure that the beam is traveling at constant height relative to the table.

6. Insert the Prism 1 Assembly into the beam path such that the beam is a few millimeters from the top of the prism and a few millimeters from the apex of the prism.

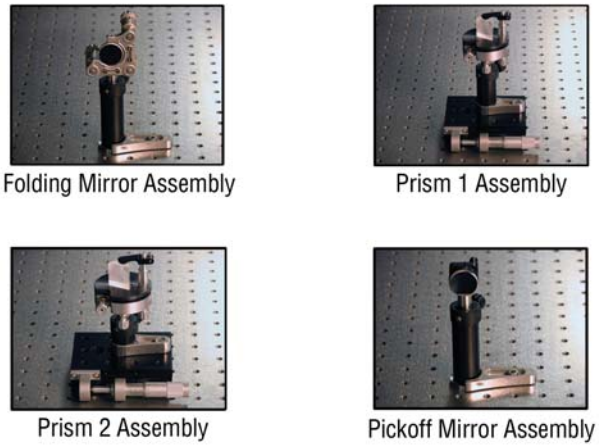

Figure 5. Diagrams of the four assemblies

7. Rotate the prism (and mount) such that the beam deviation, δ, from its unaltered path is minimized (see Figure 6). This ensures Brewster angle of incidence on the prism. Move the prism across the beam such that the beam intersects the prism as close to the apex as possible without any observable clipping.

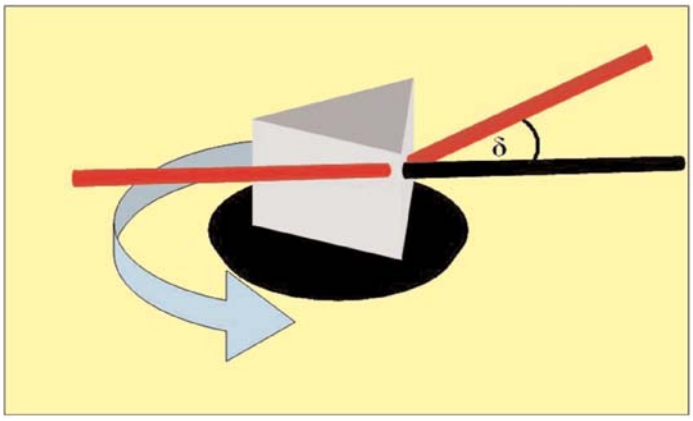

Figure 6. Diagram illustrating angle of minimum deviation

8. Using the tip/tilt adjustment on the prism table, ensure that the beam is traveling at constant height after exiting the prism.

9. Insert the Prism 2 Assembly into the beam path and secure the translation stage to the optical table. Take care that the distance between the apex of Prism 1 and the apex of Prism 2 is at least equal to the value determined in Step 3.

10. Repeat Step 7 for the Prism Assembly 2.

11. Secure the Folding Mirror Assembly after the second prism as shown in Figure 7.

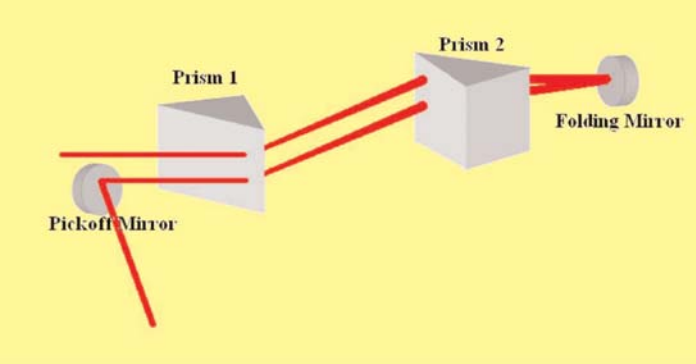

Figure 7. The prism compressor (folded geometry)

12. Send the beam back on itself with a slight horizontal displacement of a few degrees depending on the separation between prisms.
13. Install the Pickoff Mirror Assembly just prior to the Prism 1 Assembly. The top of the pickoff mirror should be as close to the incoming beam as possible.
14. Fine tune the tip/tilt adjustments on the Folding Mirror Assembly so that the beam exiting the compressor travels in the same vertical plane as the entering beam and intersects the Pickoff Mirror Assembly without clipping the top of the mirror.
15 Use the Pickoff Mirror to route the beam to an autocorrelator.
16. Using the translation stage at the base of the Prism 2 Assembly, move the prism in and out of the beam in order to minimize the pulse width. If, in the process of minimizing the pulse duration, the beam clips on the edge of the prism, increase the prism separation. If, on the other hand, the beam is coming close to the base of the prism, decrease the separation between prisms. Repeat this step until the pulse duration is minimized.

Experimental Results

1. Compression of Spectra-Physics® Broadband Tsunami® oscillator output using a LakL21 Prism Pair

In this experiment, we compress an output pulse from a Tsunami oscillator configured for broadband operation (www.newport.com\tsunami). The beam directly out of the Tsunami (approximately 2 mm diameter at $1/e^2$) is routed to the Spectra-Physics PulseScout™ autocorrelator and spectrometer (www.newport.com\pulsescout) using a silver mirror. The results of measurement as read by the PulseScout autocorrelator are shown in Figure 8.

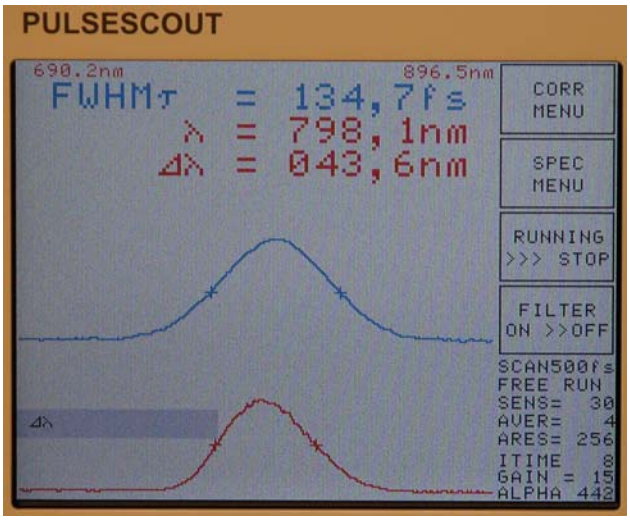

Figure 8. Bandwidth and autocorrelation trace of broadband Tsunami prior to compression

The autocorrelation width is 134 fs at FWHM and the bandwidth around 800 nm is 42 nm, FWHM. This corresponds to pulse duration of 94 fs ($\Delta t_{intensity} = \Delta t_{AC}/1.44$ for a Gaussian pulse). The transform limited pulse width is 22 fs, and from equation (9) we calculate the GDD on the pulse to be 729 fs^2. The GDD is due to the output coupler of the laser and routing optics. Solving equation (12) predicts a prism separation of 38 cm for LakL21 glass and 22 cm for SF10 glass. Experimentally, we found the optimal prism separation for LakL21 glass to be 37.0 cm with the compressed pulse duration of 26 fs (see Figure 9). When using SF10 glass prisms, we found the optimal prism separation to be 22 cm with compressed pulse duration of 32 fs. The experimental distances agree with the calculated distances to within a few percent.

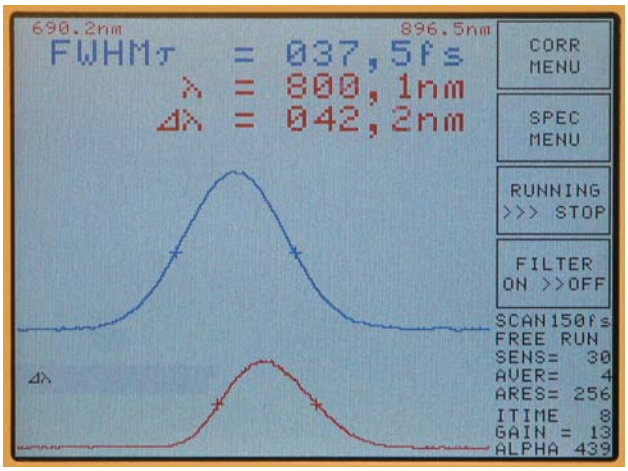

Figure 9. Bandwidth and autocorrelation trace of broadband Tsunami after compression

A prism compressor does not compensate higher order dispersion. SF10 glass has significantly more third order dispersion than LakL21, hence the compressed pulse is 20% longer when using a compressor with SF10 prisms compared to LakL21 prisms. For this reason, SF10 is not recommended for pulses below 50 fs. The PulseScout, used to collect the above autocorrelation traces, can also be used to record the fringe resolved autocorrelation trace as shown in Figure 10.

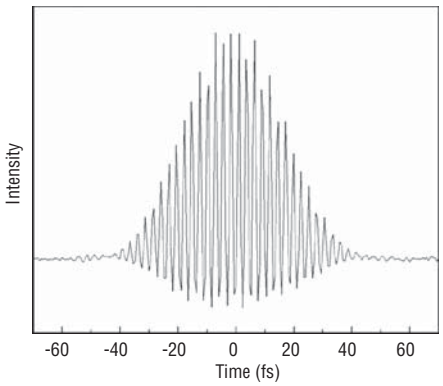

Figure 10. Fringe-resolved autocorrelation trace of compressed output from broadband Tsunami

2. Compression of the Spectra-Physics Tsunami HP using a SF10 Prism Pair

In this experiment, we demonstrate compression of the output pulse of the Tsunami HP oscillator (www.newport.com\tsunami) broadened by several optical components. The beam directly out of the Tsunami (approximately 2 mm diameter at $1/e^2$) is routed through a waveplate and polarizer providing variable attenuation of the output power (see Apps. Note 26). After the polarizer, the beam is directed to the PulseScout autocorrelator and spectrometer. We measured the autocorrelation width of 169 fs at FWHM and the bandwidth around 775 nm of 10.5 nm at FWHM. An autocorrelation width of 169 fs corresponds to a pulse duration of 120 fs. Applying the uncertainty principle, we find that the transform limited pulse width is 84 fs, and from equation (9) we find that the GDD on the pulse is 2580 fs^2. The dispersion on the pulse is due to the output coupler, waveplate, calcite polarizer, as well as the routing optics. Taking into account that $GDD_{PRISM} = -GDD_{PULSE}$, equation (12) predicts a prism separation of 30 cm for SF10 glass. Experimentally, we found the optimal prism separation for SF10 glass to be 30 cm with the compressed pulse duration of 85 fs. The experimental distance and pulse duration are in excellent agreement with the calculations. Figure 11 shows that actual prism arrangement used in the experiment.

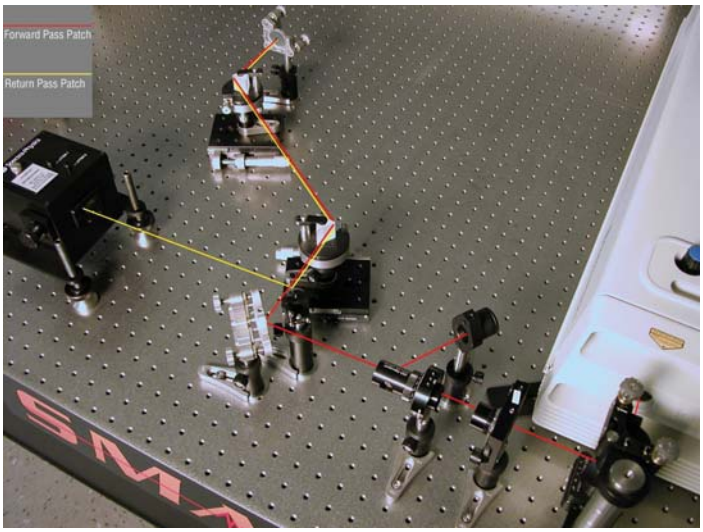

Figure 11. Prism arrangement used to compress the output of Tsunami HP

Conclusions

We demonstrated a simple and cost effective prism compressor for ultrashort laser pulses. The purpose of this compressor is to provide means of controlling dispersion of the femtosecond pulses on a typical experimental set-up that includes oscillators, amplifiers and OPAs. We also provided tables and expressions that will allow users to choose the material of the prisms and determine their optimal separation that will allow the delivery of the shortest pulses to the experiment.

Guide to Appendix 1

Appendix 1 provides a series of tables that can be used to determine the optimum prism separation for the prism compressor described above. Each table is unique for a given wavelength of light and prism material (SF10 = SF10 glass, LakL21 = LakL21 glass and FS = Fused Silica). The column header (25 fs – 200 fs) corresponds to the measured pulse width prior to compression. The row header (25 fs -200 fs [top], bandwidth [bottom]) corresponds to the actual bandwidth (bottom of row) and the transform limited pulse duration (top of row). The matrix elements describe the optimal prism separation (top) and group delay dispersion (bottom) for a combination of pulse width (measured) and bandwidth (measured).

Using the tables is fairly straightforward. For example, in the first experiment described in this note, with the laser operating at 800 nm, the measured pulse width is 94 fs. For a given material, LakL21 at 800 nm, we scroll down Column 1 to the pulse width closest to 94 fs (100 fs in this case). Then we scroll across to the column closest to the measured bandwidth (37.5 nm in this case). The corresponding matrix element then gives the approximate prism separation 41 cm and GDD 870 fs^2. The determined prism separation can serve as a good starting point for setting up and optimizing the compressor without solving the equation (12).

Alternatively, if the thickness and dispersive properties of the optical elements in the beam path are known, the GDD can be determined from Table 2 by summing the GVD multiplied by the thickness of each optic. After calculating the GDD, measure the bandwidth of the pulse. For a given material, wavelength, and bandwidth, find the matrix element with the nearest GDD. The correct prism separation is also contained in this matrix element.

Appendix 1 – Tables of Prism Parameters

SF10 – 800 nm

	25 fs (37.5 nm)	50 fs (18.8 nm)	75 fs (12.5 nm)	100 fs (9.4 nm)	125 fs (7.5bnm)	150 fs (6.3 nm)	175 fs (5.4)	200 fs (4.7 nm)
25 fs	0	0	0	0	0	0	0	0
50 fs	19 cm 390 fs^2	0	0	0	0	0	0	0
75 fs	21 cm 640 fs^2	21 cm 1010 fs^2	0	0	0	0	0	0
100 fs	22 cm 870 fs^2	25 cm 1560 fs^2	25 cm 1790 fs^2	0	0	0	0	0
125 fs	24 cm 1100 fs^2	28 cm 2070 fs^2	31 cm 2710 fs^2	30 cm 2710 fs^2	0	0	0	0
150 fs	25 cm 1330 fs^2	31 cm 2550 fs^2	36 cm 3510 fs^2	38 cm 4030 fs^2	36 cm 3740 fs^2	0	0	0
175 fs	27 cm 1560 fs^2	33 cm 3020 fs^2	40 cm 4280 fs^2	45 cm 5180 fs^2	46 cm 5520 fs^2	42 cm 4880 fs^2	0	0
200 fs	28 cm 1790 fs^2	36 cm 3490 fs^2	44 cm 5020 fs^2	51 cm 6250 fs^2	55 cm 7040 fs^2	56 cm 7160 fs^2	49 cm 6110 fs^2	0

SF10 - 550 nm

	25 fs (17.7 nm)	50 fs (8.9 nm)	75 fs (5.9 nm)	100 fs (4.4 nm)	125 fs (3.5 nm)	150 fs (3.0 nm)	175 fs (2.5 nm)	200 fs (2.2 nm)
25 fs	0	0	0	0	0	0	0	0
50 fs	10 cm 390 fs^2	0	0	0	0	0	0	0
75 fs	10 cm 640 fs^2	10 cm 1010 fs^2	0	0	0	0	0	0
100 fs	10 cm 870 fs^2	11 cm 1560 fs^2	11 cm 1790 fs^2	0	0	0	0	0
125 fs	11 cm 1100 fs^2	12 cm 2070 fs^2	13 cm 2710 fs^2	13 cm 2710 fs^2	0	0	0	0
150 fs	11 cm 1330 fs^2	13 cm 2550 fs^2	14 cm 3510 fs^2	15 cm 4030 fs^2	14 cm 3740 fs^2	0	0	0
175 fs	12 cm 1560 fs^2	14 cm 3020 fs^2	15 cm 4280 fs^2	17 cm 5180 fs^2	17 cm 5520 fs^2	16 cm 4880 fs^2	0	0
200 fs	12 cm 1790 fs^2	14 cm 3490 fs^2	17 cm 5020 fs^2	19 cm 6250 fs^2	20 cm 7040 fs^2	20 cm 7160 fs^2	18 cm 6110 fs^2	0

SF10 - 400 nm

	25 fs (9.4 nm)	50 fs (4.7 nm)	75 fs (3.1 nm)	100 fs (2.3 nm)	125 fs (1.9 nm)	150 fs (1.6 nm)	175 fs (1.3 nm)	200 fs (1.2 nm)
25 fs	0	0	0	0	0	0	0	0
50 fs	5 cm 390 fs^2	0	0	0	0	0	0	0
75 fs	5 cm 640 fs^2	5 cm 1010 fs^2	0	0	0	0	0	0
100 fs	5 cm 870 fs^2	5 cm 1560 fs^2	5 cm 1790 fs^2	0	0	0	0	0
125 fs	5 cm 1100 fs^2	5 cm 2070 fs^2	5 cm 2710 fs^2	5 cm 2710 fs^2	0	0	0	0
150 fs	5 cm 1330 fs^2	5 cm 2550 fs^2	6 cm 3510 fs^2	6 cm 4030 fs^2	6 cm 3740 fs^2	0	0	0
175 fs	5 cm 1560 fs^2	5 cm 3020 fs^2	6 cm 4280 fs^2	6 cm 5180 fs^2	6 cm 5520 fs^2	6 cm 4880 fs^2	0	0
200 fs	5 cm 1790 fs^2	6 cm 3490 fs^2	6 cm 5020 fs^2	7 cm 6250 fs^2	7 cm 7040 fs^2	7 cm 7160 fs^2	6 cm 6110 fs^2	0

LakL21 – 800 nm

	25 fs (37.5 nm)	50 fs (18.8 nm)	75 fs (12.5 nm)	100 fs (9.4 n m)	125 fs (7.5bnm)	150 fs (6.3 nm)	175 fs (5.4)	200 fs (4.7 nm)
25 fs	0	0	0	0	0	0	0	0
50 fs	30 cm 390 fs ^{2}	0	0	0	0	0	0	0
75 fs	35 cm 640 fs ^{2}	41 cm 1010 fs ^{2}	0	0	0	0	0	0
100 fs	41 cm 870 fs ^{2}	53 cm 1560 fs ^{2}	57 cm 1790 fs ^{2}	0	0	0	0	0
125 fs	46 cm 1100 fs ^{2}	64 cm 2070 fs ^{2}	76 cm 2710 fs ^{2}	75 cm 2710 fs ^{2}	0	0	0	0
150 fs	51 cm 1330 fs ^{2}	74 cm 2550 fs ^{2}	93 cm 3510 fs ^{2}	103 cm 4030 fs ^{2}	96 cm 3740 fs ^{2}	0	0	0
175 fs	56 cm 1560 fs ^{2}	84 cm 3020 fs ^{2}	108 cm 4280 fs ^{2}	126 cm 5180 fs ^{2}	133 cm 5520 fs ^{2}	119 cm 4880 fs ^{2}	0	0
200 fs	61 cm 1790 fs ^{2}	94 cm 3490 fs ^{2}	124 cm 5020 fs ^{2}	148 cm 6250 fs ^{2}	164 cm 7160 fs ^{2}	165 cm 7160 fs ^{2}	144 cm 6110 fs ^{2}	0

LakL21 -550 nm

	25 fs (17.7 nm)	50 fs (8.9 nm)	75 fs (5.9 nm)	100 fs (4.4 nm)	125 fs (3.5 nm)	150 fs (3.0 nm)	175 fs (2.5 nm)	200 fs (2.2 nm)
25 fs	0	0	0	0	0	0	0	0
50 fs	21 cm 390 fs ^{2}	0	0	0	0	0	0	0
75 fs	24 cm 640 fs ^{2}	26 cm 1010 fs ^{2}	0	0	0	0	0	0
100 fs	26 cm 870 fs ^{2}	32 cm 1560 fs ^{2}	34 cm 1790 fs ^{2}	0	0	0	0	0
125 fs	29 cm 1100 fs ^{2}	37 cm 2070 fs ^{2}	43 cm 2710 fs ^{2}	42 cm 2710 fs ^{2}	0	0	0	0
150 fs	31 cm 1330 fs ^{2}	42 cm 2550 fs ^{2}	51 cm 3510 fs ^{2}	55 cm 4030 fs ^{2}	52 cm 3740 fs ^{2}	0	0	0
175 fs	34 cm 1560 fs ^{2}	47 cm 3020 fs ^{2}	58 cm 4280 fs ^{2}	66 cm 5180 fs ^{2}	69 cm 5520 fs ^{2}	63 cm 4880 fs ^{2}	0	0
200 fs	36 cm 1790 fs ^{2}	51 cm 3490 fs ^{2}	65 cm 5020 fs ^{2}	77 cm 6250 fs ^{2}	84 c m 7040 fs ^{2}	85 cm 7160 fs ^{2}	75 cm 6110 fs ^{2}	0

LakL21 -400 nm

	25 fs (9.4 nm)	50 fs (4.7 nm)	75 fs (3.1 nm)	100 fs (2.3 nm)	125 fs (1.9 nm)	150 fs (1.6 nm)	175 fs (1.3 nm)	200 fs (1.2 nm)
25 fs	0	0	0	0	0	0	0	0
50 fs	11 cm 390 fs ^{2}	0	0	0	0	0	0	0
75 fs	12 cm 640 fs ^{2}	13 cm 1010 fs ^{2}	0	0	0	0	0	0
100 fs	13 cm 870 fs ^{2}	15 cm 1560 fs ^{2}	16 cm 1790 fs ^{2}	0	0	0	0	0
125 fs	14 cm 1100 fs ^{2}	17 cm 2070 fs ^{2}	19 cm 2710 fs ^{2}	19 cm 2710 fs ^{2}	0	0	0	0
150 fs	15 cm 1330 fs ^{2}	19 cm 2550 fs ^{2}	22 cm 3510 fs ^{2}	24 cm 4030 fs ^{2}	22 cm 3740 fs ^{2}	0	0	0
175 fs	16 cm 1560 fs ^{2}	20 cm 3020 fs ^{2}	25 cm 4280 fs ^{2}	28 cm 5180 fs ^{2}	29 cm 5520 fs ^{2}	26 cm 4880 fs ^{2}	0	0
200 fs	17 cm 1790 fs ^{2}	22 cm 3490 fs ^{2}	27 cm 5020 fs ^{2}	31 cm 6250 fs ^{2}	34 cm 7040 fs ^{2}	34 cm 7160 fs ^{2}	31 cm 6110 fs ^{2}	0

FS – 800 nm

	25 fs (37.5 nm)	50 fs (18.8 nm)	75 fs (12.5 nm)	100 fs (9.4 nm)	125 fs (7.5bnm)	150 fs (6.3 nm)	175 fs (5.4)	200 fs (4.7 nm)
25 fs	0	0	0	0	0	0	0	0
50 fs	49 cm 390 fs ^{2}	0	0	0	0	0	0	0
75 fs	62 cm 640 fs ^{2}	77 cm 1010 fs ^{2}	0	0	0	0	0	0
100 fs	74 cm 870 fs ^{2}	103 cm 1560 fs ^{2}	113 cm 1790 fs ^{2}	0	0	0	0	0
125 fs	85 cm 1100 fs ^{2}	128 cm 2070 fs ^{2}	156 cm 2710 fs ^{2}	155 cm 2710 fs ^{2}	0	0	0	0
150 fs	97 cm 1330 fs ^{2}	151 cm 2550 fs ^{2}	195 cm 3510 fs ^{2}	218 cm 4030 fs ^{2}	203 cm 3740 fs ^{2}	0	0	0
175 fs	108 cm 1560 fs ^{2}	174 cm 3020 fs ^{2}	231 cm 4280 fs ^{2}	272 cm 5180 fs ^{2}	287 cm 5520 fs ^{2}	256 cm 4880 fs ^{2}	0	0
200 fs	120 cm 1790 fs ^{2}	197 cm 3490 fs ^{2}	266 cm 5020 fs ^{2}	323 cm 6250 fs ^{2}	358 cm 7040 fs ^{2}	363 cm 7160 fs ^{2}	313 cm 6110 fs ^{2}	0

FS - 550 nm

	25 fs (17.7 nm)	50 fs (8.9 nm)	75 fs (5.9 nm)	100 fs (4.4 nm)	125 fs (3.5 nm)	150 fs (3.0 nm)	175 fs (2.5 nm)	200 fs (2.2 nm)
25 fs	0	0	0	0	0	0	0	0
50 fs	37 cm 390 fs ^{2}	0	0	0	0	0	0	0
75 fs	43 cm 640 fs ^{2}	50 cm 1010 fs ^{2}	0	0	0	0	0	0
100 fs	49 cm 870 fs ^{2}	64 cm 1560 fs ^{2}	69 cm 1790 fs ^{2}	0	0	0	0	0
125 fs	55 cm 1100 fs ^{2}	77 cm 2070 fs ^{2}	91 cm 2710 fs ^{2}	91 cm 2710 fs ^{2}	0	0	0	0
150 fs	62 cm 1330 fs ^{2}	89 cm 2550 fs ^{2}	111 cm 3510 fs ^{2}	123 cm 4030 fs ^{2}	115 cm 3740 fs ^{2}	0	0	0
175 fs	68 cm 1560 fs ^{2}	101 cm 3020 fs ^{2}	130 cm 4280 fs ^{2}	151 cm 5180 fs ^{2}	159 cm 5520 fs ^{2}	143 cm 4880 fs ^{2}	0	0
200 fs	73 cm 1790 fs ^{2}	113 cm 3490 fs ^{2}	148 cm 5020 fs ^{2}	177 cm 6250 fs ^{2}	196 cm 7040 fs ^{2}	198 cm 7160 fs ^{2}	172 cm 6110 fs ^{2}	0

SF - 400 nm

	25 fs (9.4 nm)	50 fs (4.7 nm)	75 fs (3.1 nm)	100 fs (2.3 nm)	125 fs (1.9 nm)	150 fs (1.6 nm)	175 fs (1.3 nm)	200 f s (1.2 nm)
25 fs	0	0	0	0	0	0	0	0
50 fs	20 cm 390 fs ^{2}	0	0	0	0	0	0	0
75 fs	22 cm 640 fs ^{2}	25 cm 1010 fs ^{2}	0	0	0	0	0	0
100 fs	24 cm 870 fs ^{2}	30 cm 1560 fs ^{2}	32 cm 1790 fs ^{2}	0	0	0	0	0
125 fs	27 cm 1100 fs ^{2}	35 cm 2070 fs ^{2}	41 cm 2710 fs ^{2}	40 cm 2710 fs ^{2}	0	0	0	0
150 fs	29 cm 1330 fs ^{2}	40 cm 2550 fs ^{2}	48 cm 3510 fs ^{2}	53 cm 4030 fs ^{2}	50 cm 3740 fs ^{2}	0	0	0
175 fs	31 cm 1560 fs ^{2}	44 cm 3020 fs ^{2}	56 cm 4280 fs ^{2}	64 cm 5180 fs ^{2}	67 cm 5520 fs ^{2}	60 cm 4880 fs ^{2}	0	0
200 fs	34 cm 1790 fs ^{2}	49 cm 3490 fs ^{2}	63 cm 5020 fs ^{2}	74 cm 6250 fs ^{2}	81 cm 7040 fs ^{2}	82 cm 7160 fs ^{2}	72 cm 6110 fs ^{2}	0

References

1. J. Diels and W. Rudolf, *Ultrashort Laser Pulse Phenomena*, Second Edition (Massachusetts, Academic Press, 2006).
2. E. Oran Brigham, *The Fast Fourier Transform: An Introduction to Its Theory and Application* (New Jersey, Prentice Hall, 1973).
3. R. Trebino, *Frequency-Resolved Optical Gating: The Measurement of Ultrashort Laser Pulse* (Massachusetts, Kluwer Academic Publishers, 2002).
4. R.L. Fork, O.E. Martinez, and J.P. Gordon, (Opt. Lett. 9, 150 1984).
5. R.E. Sheriff, (J. Opt. Soc. Am. B 15, 1224 1998).

Parts List

Description	Quantity	Newport Part Number
Pick-off Mirror Assembly		
Broadband (480-2000 nm) Mirror, Protected Silver Coating	1	10D20ER.2
Ultima® Kinematic Optical Mount, 0.5 in. Platform	1	U50-P
Ultima® Mirror Holder, 1"	1	UPA1
Post, 2 in.	1	SP-2
Post Holder, 2 in.	1	VPH-2-P
Clamping Fork	1	PS-F
Adjustable Prism Assemblies		
Ultrafast Laser Dispersion Prism, LaKL21, grade AA	2	10LK10
Ultima® Gimbal Prism Mount	2	UGP-1
Vernier Micrometer, 50 mm Travel	2	SM-50
Low-Profile Linear Translation Stage	2	433
Post, 1 in.	2	SP-1
Post Holder, 1 in.	2	VPH-1
Slotted Base	2	B-05A
Folding Mirror Assembly		
Broadband (480-2000 nm) Mirror, Protected Silver Coating	1	10D20ER.2
Suprema® Kinematic Optical Mounts	1	SN100-F2KN
Post, 3 in.	1	SP-3
Post Holder, 3 in.	1	VPH-3-P
Clamping Fork	1	PS-F

Description	Quantity	Newport Part Number
Note: Prism selection is dependent upon input wavelength and application. The following set of prisms would replace P.N. 10LK10 under certain scenarios.		
Ultrafast Laser Dispersion Prism, SF10	2	10SF10
Ultrafast Laser Dispersion Prism, UV grade Fused Silica	2	10SB10
Note: 1in. Posts and Post Holders on the Prism Assemblies will accommodate an optical axis height between 4 in.-4.75 in.. The Mai Tai has an optical height of 4.375 in.. By substituting 2 in. Posts and 2 in. Post Holders, the Prism Assemblies will accommodate an optical axis height between 5 in.-6.75 in.. The Tsunami has an optical height of 5.5 in. and the Spitfire Amplifier has an optical height of 6.25 in.		
Post, 2 in.	2	SP-2
Post Holder, 2 in.	2	VPH-2

Newport Corporation

Worldwide Headquarters
1791 Deere Avenue
Irvine, CA 92606

(In U.S.): 800-222-6440
Tel: 949-863-3144
Fax: 949-253-1680

Internet: sales@newport.com

Newport
Experience | Solutions

Spectra-Physics
A Division of Newport Corporation

Visit Newport Online at: **www.newport.com**

ISO 9001
FM 27207

Newport Corporation, Irvine, California, has been certified compliant with ISO 9001 by the British Standards Institution.

MM#90000089
DS-11065